Structure and morphology of the Ag/MgO(001) interface during *in situ* growth at room temperature

O. Robach, G. Renaud,* and A. Barbier
CEA-Grenoble, Département de Recherche Fondamentale sur la Matière Condensée/SP2M/IRS, 17, rue des Martyrs, 38054 Grenoble Cedex 9, France

(Received 1 June 1998; revised manuscript received 14 December 1998)

The structure and morphology of Ag deposits grown at room temperature on high-quality MgO(001) surfaces have been investigated *in situ*, from 0.2 to 300 equivalent monolayers (ML) of Ag deposited. Surface x-ray diffraction and grazing incidence small angle x-ray scattering parallel and perpendicular to the surface were combined. Nucleation, growth, and coalescence of islands are found from 0.2 ML. The average in-plane width, height, and in-plane separation of growing islands are deduced and are found to reproduce well the Mg 1*s* x-ray photoemission spectroscopy spectrum previously reported by other authors. The height over width ratio of the islands is $\sim 0.37 \pm 0.05$ at all stages of the deposit. Ag grows in cube-on-cube epitaxy with respect to the MgO(001) substrate. A very unusual evolution of the state of strain in Ag with increasing amount of Ag deposited is observed. Below 4–6 ML (island width smaller than 90 Å), the small Ag islands are coherent with the MgO. Below 1 ML (island width smaller than 35 Å), they have their bulk lattice parameter, and between 1 and 4 ML they become more and more strained by the MgO substrate, with an average lattice parameter intermediate between those of Ag and of MgO. Around 4–6 ML, the islands reach a critical size and misfit dislocations are introduced at the edges. Above 30 ML, the film is almost continuous, and the interfacial misfit dislocations reorder to form a square network, oriented along ⟨110⟩ directions. Stacking faults appear in Ag at this stage. A small amount of twinned Ag also starts to grow around 4 ML. This unusual evolution of the strain in the Ag islands and the following introduction of misfit dislocations are interpreted on the basis of a one-dimensional Frenkel-Kontorova model involving a very weak Ag-MgO interaction and a weak corrugation of the interatomic potential. Quantitative measurements and analysis of the MgO crystal truncation rods (CTR's) during growth were shown to provide different structural parameters of the interface that are important for theoretical calculation, especially the epitaxial site, above oxygen atoms of the substrate, and the interfacial distance (2.52 ± 0.1 Å). The origin of the interference along the CTR's is discussed according to the strain state of the epitaxial Ag. [S0163-1829(99)14131-6]

I. INTRODUCTION

Metal-ceramic interfaces are present in numerous technological areas, such as thin films, composite materials, microelectronics, catalysis, and protection against corrosion or industrial glasses. The thermal, mechanical, chemical, or electrical properties of these materials often depend on the atomic structure of the metal/ceramic interface they contain. From a theoretical point of view, the properties of metal-oxide interfaces are difficult to predict because the interaction is very complex at the atomic level.[1–3] The interfacial energy contains several terms[4] that are of the same order of magnitude. Their relative weights are difficult to estimate because of the lack of experimental data. The Ag/MgO(001) interface has been chosen by numerous theoreticians as a prototypical metal-oxide system[5] because it is relatively simple. It has a fourfold symmetry, Ag is a noble metal and hence, no chemical reaction takes place at the interface; the epitaxy is cube-on-cube,[6–8] and the contribution of epitaxial strains to the interfacial energy is often neglected, because of the moderate lattice parameter mismatch, -2.98%, between fcc Ag and rocksalt MgO. Moreover, the MgO(001) surface relaxation is very small,[9] and thus the surface can be considered as a simple truncation of the bulk. Two important questions for theoreticians are the determination of the adsorption site among the three possible ones: above O ions of the substrate, above Mg ions, or in between, above the ''octahedral site,'' and the determination of the interfacial distance between the last MgO(001) plane and the first Ag(001) plane.

The experimental determination of these two interfacial parameters, and more generally, of the structure and morphology of the Ag/MgO(001) interface during the growth, is thus very important to test the theories. However, the Ag/MgO(001) system is experimentally difficult to study because only few characterization techniques can be used. The charge build-up effects due to the insulating character of the substrate and the weak adhesion of Ag handicap most investigations. The intrinsic structure and morphology of Ag deposits on MgO(001) are also difficult to determine because they are very sensitive to the preparation of the MgO(001) surface. For example, the amount of Ag in cube-on-cube epitaxy strongly decreases if the substrate temperature is higher than 50 °C or if the surface is slightly contaminated by C or Ca.[10] This may explain why different studies[2,11] disagree on the growth mode of Ag on MgO at room temperature (RT).

Moreover, very little is known on the processes of relaxation of the lattice parameter misfit between Ag and MgO. Although some studies claimed an initial two-dimensional (2D) growth, according to most investigations, the growth is of the Volmer-Weber type (i.e., 3D), and for thick deposits,

the misfit is known to be relaxed by an ordered array of interfacial misfit dislocations.[12,13] An important question is thus to analyze the way the Ag lattice is ''connected'' to the MgO one during cluster growth; what is the residual strain in Ag and its evolution. In particular, what are the processes involved in the transformation from an coherent to an incoherent island. We call ''coherent'' an island that is free from interfacial dislocations, i.e., it has N Ag planes ''connected'' to N MgO planes at the interface. By contrast, an incoherent island contains interfacial defects such as stacking faults or dislocations. Note that, in a coherent island, the adsorbate atoms in the first plane are not necessarily exactly above the substrate sites, but their in-plane displacement with respect to the substrate sites should not exceed half the in-plane distance between these sites. Hence, an island can be coherent with the MgO only if its lateral size is smaller than a given critical size (except if the Ag in the island is strained to the MgO in-plane lattice parameter). This definition implies that there exists a preferential adsorption site for the Ag on the MgO surface.

Finally, it is important to analyze how the ultimate misfit dislocation network is constructed. The mechanism by which dislocations are introduced is very well known in the case of the growth of a 2D fully strained film, but it is much less well known in the present case of 3D relaxed growth, although it was described in the seventies by Van der Merwe.[14] In the case of the growth of a 2D fully strained film, which happens when the adsorbate-substrate interaction is strong, the introduction of the misfit dislocations corresponds to a ''cracking'' of the film, with an extended reorganization of the adsorbate-adsorbate and adsorbate-substrate bonds. The elastic energy stored in the strained film increases proportionally to its thickness, up to a point where it is energetically more favorable to relax the misfit by dislocations. In the case of 3D growth of a partially strained or relaxed adsorbate, the sole increase of the islands width naturally leads to a critical size for which dislocations are introduced at the edges. We will see that this is the case for the Ag/MgO system.

Grazing incidence x-ray scattering[15] (GIXS) and grazing incidence small angle x-ray Scattering[11,16,17] (GISAXS) are well suited for characterizing the structure and morphology of metal/oxide interfaces during their growth by molecular-beam epitaxy, because they are insensitive to the insulating character of the substrate and they can be used *in situ*, in ultra-high vacuum (UHV).

This paper presents GIXS and GISAXS results on the growth of Ag on MgO(001) at room temperature (RT). The experimental conditions are first described (Sec. II). The results are then presented (Sec. III). A first subsection (III A) concerns the morphology and structure of the deposit. The strain state at the Ag/MgO interface, of which a short account was given in a previous letter,[18] is discussed in a second subsection (III B). A third subsection (III C) presents a detailed analysis of the evolution of the MgO(001) crystal truncation rods[19,20] (CTR's) during growth, allowing the determination of the epitaxial site and interfacial distance. Combining the information given by the different measurements finally allows to propose a new description of the growth mode of Ag on MgO. Possible mechanisms at the Ag-MgO interface leading to this growth mode are discussed in Sec. IV. The conclusion follows.

II. EXPERIMENTS

The GIXS and GISAXS experiments were performed using the SUV surface diffraction setup of the BM32 CRG/IF (Collaborating Research Group / Interfaces) beamline at ESRF (European Synchrotron Radiation Facility, Grenoble, France).[21] The UHV chamber (base pressure 2.10^{-11} mbar), equipped with two Be windows, is mounted on a six-circle diffractometer of ''z-axis'' type, which allows to perform simultaneously the deposits and the diffraction measurements. This chamber is also equipped with an electronic bombardment furnace, an ion gun, reflection high-energy electron diffraction and Auger electron spectroscopy systems, and several molecular-beam epitaxy cells. Ag was deposited by means of a Knudsen cell, with a deposition rate of 0.36 monolayer (ML)/min (i.e., 0.73 Å/min) calibrated with a quartz microbalance prior and after the x-ray measurements.

The preparation of the MgO(001) substrate has been described in detail elsewhere.[9] It leads to MgO(001) surfaces that are very flat and of high-crystalline quality, free from any impurity, with in-plane domain size larger than 1 μm, average terrace size of 6000 Å, and a rms roughness of 2.4 Å. These surfaces are therefore almost ideal, so that one can expect the growth of Ag to proceed in a way as close as possible to the ''intrinsic'' one.

The measurements were performed on cumulative Ag deposits, the growth being interrupted during the measurements. The Miller indexes ($H\,K\,L$) are expressed in reciprocal lattice units (r.l.u) of MgO, using the bulk fcc unit cell ($a_{\mathrm{MgO}}=4.2119$ Å). The L index corresponds to the component of the momentum transfer perpendicular to the surface.

For the GIXS measurements, the x-ray beam energy was set at 18 keV. This high energy allows measurements of crystal truncation rods (CTR's) over a large range of perpendicular momentum-transfer values. The incident angle of the x-ray beam with respect to the surface was set at 0.08°, i.e., $\frac{2}{3}$ of the critical angle for total external reflection of MgO. This was mandatory to minimize the background arising from Compton scattering and from point defects in the bulk. The x-ray beam was focused both horizontally (H) and vertically (V), with a full width at half maximum (FWHM) of 0.42-mm (H)×0.39-mm (V) and a divergence of 1.3-mrad (H)×62-μrad (V). The sample surface was vertical. The opening of the two pairs of detection slits was fixed at 1-mm (H)×1-mm (V) (corresponding to an angular acceptance of 0.11°) for the measurements of the MgO CTR's. They were set at 1-mm (V)×6-mm (H) for in-plane measurements.

GISAXS measurements during growth were performed three times to test different experimental setups. A first measurement was performed with a standard scintillator detector, with an angular acceptance fixed at 0.33 mrad by a slit in the vertical direction and integration of the GISAXS signal in the horizontal direction, perpendicular to the surface. Two measurements were performed with a position-sensitive gas-filled detector of 100-μm resolution, located at 500 mm from the sample. In all three cases, the x-ray beam energy was fixed at 13 keV. The incident angle was set at 0.2°, slightly

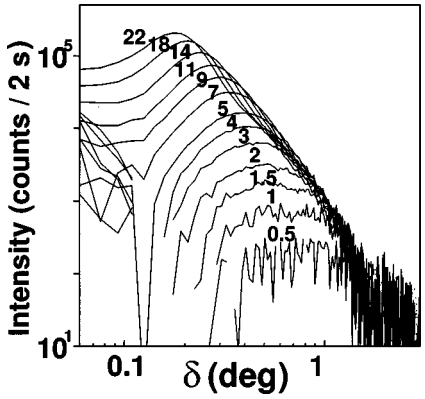

FIG. 1. In-plane GISAXS data during room temperature growth of Ag on MgO(001). The logarithm (with base 10) (Ref. 56) of the intensity, measured with a scintillator detector, is reported as a function of the logarithm (Ref. 56) of the in-plane scattering angle δ. The amount θ of deposited Ag in equivalent ML is indicated above the corresponding curve. The intensity measured on the clean MgO(001) substrate was subtracted.

above the critical angle for total external reflection of MgO (0.17° at this energy).[16] The beam was collimated in the vertical direction, with a residual divergence of 4 μrad, and focused in the horizontal direction. Its size at the sample position was reduced to 35-μm (H)×200-μm (V) by several presample slits. A lead beam stop located just after the exit beryllium window was used to stop the beam transmitted through and the beam reflected by the sample.

III. RESULTS AND ANALYSIS

A. Structure and morphology of the deposit

1. Small angle scattering: morphology

Let us first present the GISAXS data at different stages of the growth, which yield information on the morphology of the Ag deposit. Figure 1 shows in-plane GISAXS measurements with the scintillator detector from $\theta=0$ to $\theta=22$ ML, where θ is the amount of deposited Ag. The evolution is typical of a process of nucleation, growth, and coalescence of islands.[16] Small angle scattering is already found for $\theta=0.5$ ML, which shows that islands are present in the Ag deposit from the very beginning of deposition. For all θ, the intensity has a clear maximum at a finite value δ_{MAX} of the in-plane detector angle, which shows that the in-plane positions of the islands are correlated. The average in-plane interislands distance D (Fig. 2) is approximately given by $D=\lambda/\delta_{MAX}$ where λ is the x-ray wavelength. The three measurements, one with a scintillator detector, and two with a position-sensitive detector, yield a very similar increase of D with θ [Fig. 2(b)].

Previous investigations concluded to different growth modes (3D or Volmer-Weber,[22,23] 2D then 3D or Frank van der Merwe[24–26]). It is thus important to estimate the fraction of Ag that is in 3D form, in order to determine if all the deposit is 3D or if a 2D fraction can also be present at the beginning of the growth, that would not be detectable with GISAXS. For that sake, we need to estimate the average island shape and size.

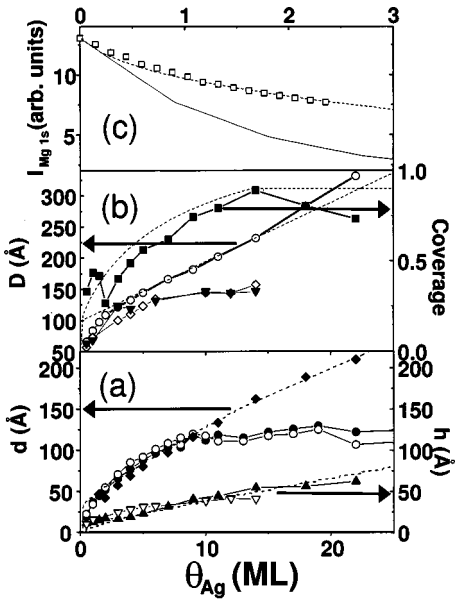

FIG. 2. (a) Left scale: average in-plane width d of Ag islands as a function of the amount θ of deposited Ag in equivalent ML, deduced from in-plane GISAXS data using an empirical determination (solid diamonds). It is compared to the average in plane domain size deduced from the FWHM $\Delta\omega$ of the rocking scans around the Ag (2.06 2.06 0) (solid circles) and (2.06 0 0) (open circles) Bragg peaks. These scans were fitted with Lorentzian distributions. The in-plane domain size is given by: $2\pi/\Delta Q_{\parallel}$ where $\Delta Q_{\parallel}=Q_{\parallel}.\Delta\omega$, $Q_{\parallel}$ being the in-plane component of the momentum transfer. The dashed line shows the width of the islands (modeled as truncated pyramids) used to calculate the XPS curve. Right scale: average island height as a function of θ, as deduced from two independent out-of-plane GISAXS measurements using a position-sensitive detector (solid and open triangles). The dashed line shows the height of the islands used to calculate the XPS curve. (b): Left scale: Evolution of the average in-plane interislands distance D with the amount θ of deposited Ag (in equivalent ML). The results of three different measurements are reported (open circles with a scintillator detector; solid triangles and open diamonds with a position-sensitive detector). The dashed line shows the interislands distance used to calculate the XPS curve. Right scale: fraction of the MgO surface that is covered by Ag (i.e., coverage) as a function of θ (solid squares), compared with the coverage used to calculate the XPS curve (dashed line). (c): Evolution of the Mg 1s XPS line (open squares) during the RT growth of Ag on MgO(001) (from Ref. 24), compared to layer by layer growth (solid line) and a calculation using a model of truncated pyramids, (Ref. 33) with $h(\theta)=0.75\theta+13.5$ and $k(\theta)=1.50+10$ (dashed line).

Let us begin with the island size. The evolution of the average in-plane island width d was deduced by an empirical method,[27] in which it is given by $d=1.916/Q_{\parallel}^{c}$, where $Q_{\parallel}^{c}$ is the momentum transfer value at which the intensity on the right of the GISAXS peak is 8% of the maximum.[28] This location is attributed to that of the first zero of the first-order Bessel function. The island width [Fig. 2(a)] is found to increase steadily between 0 and 22 ML. The average island height was deduced from out-of-plane GISAXS data, recorded with the position-sensitive detector. Figure 3 shows as an example the scattered intensity as a function of the perpendicular momentum transfer $Q_{\perp}$, for an amount $\theta=6$ ML of deposited Ag, after integration parallel to the sur-

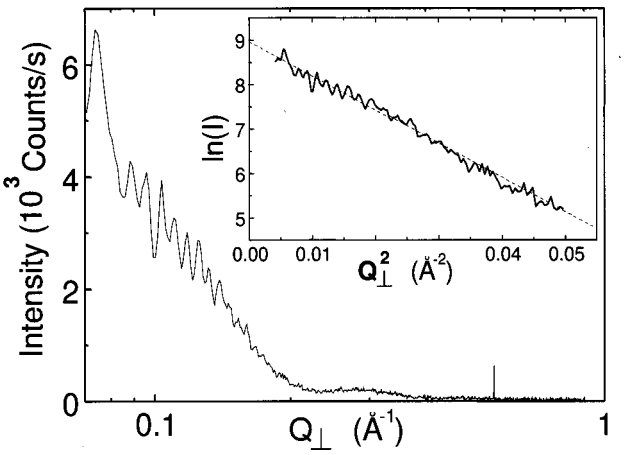

FIG. 3. GISAXS intensity as a function of the logarithm (Ref. 56) of the perpendicular momentum transfer, after integration parallel to the plane, for an equivalent amount of Ag deposited of 6 ML. The origin of the oscillations of the intensity is not understood. In the inset, the natural logarithm of the intensity closest to the origin is reported as a function of the square of the perpendicular momentum transfer. The linear trend shows that the Guinier law can be used to deduce the average island height.

face. Perpendicular to the surface, the islands are not correlated, and hence the Guinier law is valid. This is confirmed (Fig. 3) for all deposits by plotting the logarithm of the intensity as a function of $Q_\perp^2$. The evolution of the average island height as a function of θ is reported in Fig. 2(a) for two independent measurements. It increases steadily with θ, approximately proportionally to the island width. This allows to deduce the height-to-width ratio of the islands, which varies between 0.3 and 0.42 with an average value of 0.37 ± 0.05.

For estimating the amount of 3D Ag, we need to estimate the shape of the Ag islands. Unfortunately, to our knowledge, nothing is known on the exact island shape for RT growth. Information is available only for higher substrate temperature.[29,30,12,31,32] Since x-ray scattering realizes an average over all islands and since no signal specific of facets was detected at wide angles, it is not possible to assign a particular shape to the average island. In order to get a rough estimate of the amount of Ag on these islands, we considered a hexagonal packing of truncated spheres of 0.37 aspect ratio, with an interisland distance D. Below 10 ML, the Ag amount obtained with this calculation is very close to the total amount deposited. This supports a model of 3D growth without 2D fraction.

With these assumed islands shape and distribution, the fraction of the MgO(001) surface that is covered, i.e., the coverage, can be estimated. Figure 2(b) shows that already $\sim$20% of the surface is covered for small θ (<2 ML). The coverage next increases continuously to reach a maximum of $\sim$0.9 for $\theta = 14$ ML. Interestingly, very small angle scattering appears in the GISAXS data around this deposited amount, revealing the presence of large islands whose positions are no more correlated. This likely results from the beginning of the percolation of the islands [see Fig. 2(b)].

In order to check the validity of these results, we used a recently described quantitative description of the 3D growth[33] to reanalyze previously published raw Mg 1s x-ray photoemission spectroscopy (XPS) data during RT growth of Ag on cleaved MgO(001) substrates.[24] Based on qualitative arguments, the original interpretation[24] was initial 2D growth of Ag, followed by 3D growth. Using the generalized model,[33] we found that, in order to reproduce simultaneously the GISAXS and XPS data, the clusters had to be described by truncated pyramids limited by facets tilted by 45° with respect to the (001) plane. This is consistent with the cube-on-cube epitaxy. The parameters of the model were the uncoverable part of the surface ϵ, the truncation height k, of the pyramids (i.e., k levels starting from the top of the pyramids are not occupied by atoms) and h, which is such that $2(h+k)$ is the separation between the centers of two neighboring pyramids. The value of ϵ is directly given by the evolution of the coverage, $\epsilon = 0.1$, i.e., 10% of the surface is never covered by the Ag overlayer, which was confirmed by scanning electron microscopy inspection of 1500 Å-thick deposits. In order to reproduce all the GISAXS and XPS data, h and k had to be left linearly dependent on the thickness θ. A very good agreement with all these data from different experiments [see Fig. 2(c)] was obtained for the following laws: $h(\theta) = 0.75\theta + 13.5$ and $k(\theta) = 1.5\theta + 10$. Physically this means that the growth is always 3D since $h(0) = 13.5$ and $k(0) = 10$ (a layer-by-layer growth corresponds to $h = 1$ and $k = 0$) although during the completion of the first layer of the truncated pyramids a small quantity of Ag will grow like a 2D layer. The general shape of the islands is given by the truncated pyramid but the morphology of the islands changes continuously during the growth: the island density decreases (h increases) and the top of the islands becomes larger and larger (k increases). Within this model all available data are reproduced (Fig. 2) without any additional parameter. This description corresponds naturally to a nucleation, growth and continuous coalescence process.

In summary, the growth is 3D from the very beginning, and the average height-to-width ratio of the islands is of the order of 0.37 ± 0.05.

2. Wide angle scattering: structure and morphology

Figure 4 shows radial GIXS measurements along the (H 0 0.1) and (H H 0.1) directions. These scans cross the MgO CTR's and Ag rods at $H = 2$ and $H = 2.06$, respectively. For all deposited amounts, scattering is observed near the location for relaxed Ag ($H \sim 2.062$), which shows that Ag in cube-on-cube epitaxy is present, and that it is at least partially relaxed.

Comparison between the widths of rocking scans around the (220) and (200) Ag Bragg peaks shows that these widths are dominated by the finite domain size effect: the broadening due to in-plane mosaic spread is negligible. The average in-plane domain size deduced from these measurements is compared in Fig. 2(a) to the average in-plane island size. Remarkably, the island width and the in-plane domain size are nearly identical up to $\theta = 10$ ML. Above, the domain size progressively saturates around 120–130 Å. This saturation will be discussed later.

Combining these results with the GISAXS ones shows that the major part of Ag is in cube-on-cube epitaxy and in the form of islands.

As already mentioned in a previous letter,[8] from 4 ML, twinned Ag was also detected, but in a much smaller amount

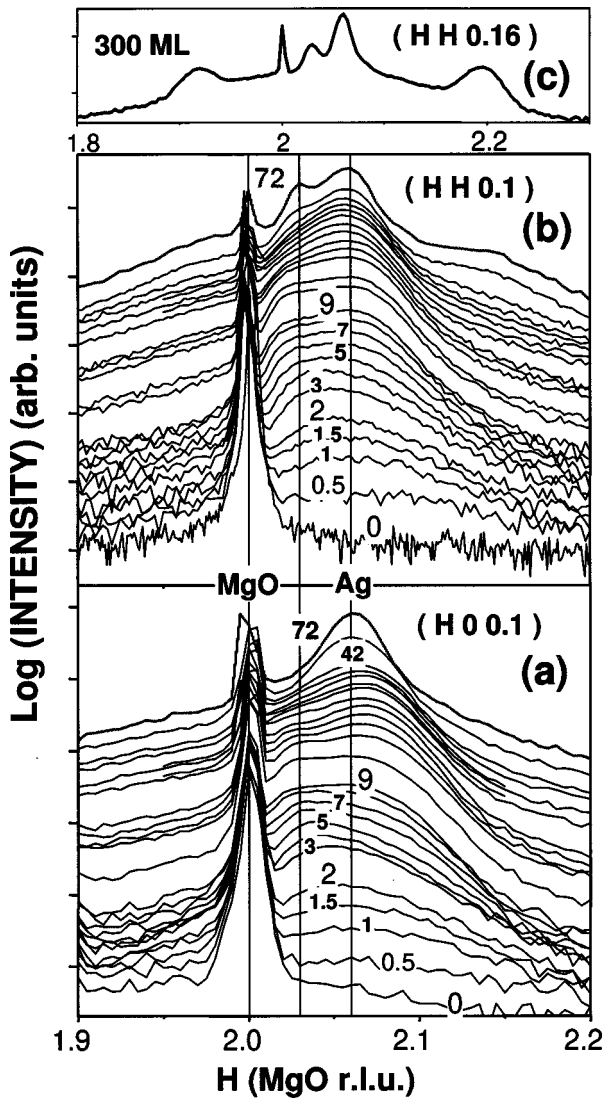

FIG. 4. Radial scans during room-temperature growth of Ag on MgO(001), measured at $L=0.1$ along the (H 0 0.1) (a) and (H H 0.1) (b) directions, as a function of the amount of deposited Ag. The logarithm (Ref. 56) of the intensity is plotted versus H. The different amounts, 0, 0.5, 1, 1.5, 2, 3, 4, 5, 6, 7, 8, 9, 10, 11, 13, 15, 17, 19, 22, 25, 28, 32, 36, 42, and 72 ML, are indicated above the corresponding curves. The second scan at 72 ML (thick line) was done with an opening of the vertical exit slits of 0.5 mm instead of 1 mm. The curves corresponding to the different deposits have been shifted vertically for clarity. Vertical lines indicate the $H=2$, $H=2.03$, and $H=2.06$ positions. Above 10 ML, the incident angle was increased in order to compensate for the refraction effects. It was fixed at 0.08° from 0 to 9 ML, at 0.12° for 10 and 11 ML, at 0.15° from 13 to 19 ML, and at 0.22° from 22 ML. A scan measured at $L=0.16$ along the (H H 0.16) direction is also shown (c) for $\theta=300$ ML, clearly revealing the dislocation peak and the two shoulders, symmetrical with respect to the Ag peak, arising from rods of scattering from stacking faults in Ag. This scan was performed with an incident angle of 0.25° and exit slits at 0.5-mm (V)×2-mm (H).

than Ag in continuity with the MgO stacking. Its growth was monitored by performing rocking scans around the (020) Bragg peak for twinned Ag, which is located at (H K L) = (1.37 0.69 1.37) for Ag twinned along the $(1\bar{1}1)$ planes.[13] Stacking faults in Ag were also found to appear from 10 ML.[18] These stacking faults produce rods of scattering oriented along the ⟨111⟩ (Ref. 34) directions, which cross the scan of Fig. 4(b) at $H=1.96$ and $H=2.16$.[35] The resulting peaks are clearly visible on the scan performed at 300 ML [Fig. 4(c)] for $L=0.16$, in which the stacking fault rods appear at $H=1.92$ and $H=2.2$.

B. Strain evolution in Ag islands

1. Qualitative description

From the preceding section it appears that the major part of Ag is in cube-on-cube epitaxy with a lattice parameter close to that of bulk Ag. For estimating the strength of the Ag-MgO interaction, an important question is how the Ag islands are connected to the substrate at the different stages of the deposit. Are the Ag islands ''floating'' on the MgO surface without being influenced by the lateral position of the atoms in the MgO, or are there strains reflecting the fact that the Ag atoms of the first plane undergo an attractive force toward a particular adsorption site of the MgO, and the fact that Ag has a different lattice parameter than MgO?

This information can be deduced by analyzing the evolution of the position (which gives the average in-plane lattice parameter), the width and the shape of the Ag scattering along radial scans (Fig. 4). The strain evolution in the Ag deposit can then be decomposed into three stages, schematically shown in Fig. 5.

1.1. Stage a: Coherent islands

At 0.5 ML, the Ag scattering is centered on $H=2.06$, showing that the Ag has, on the average, its bulk lattice parameter, as if the deposited Ag was not ''feeling'' the presence of the MgO. Between 0.5 and 4 ML, the Ag islands become progressively strained by the substrate, with an average lattice parameter intermediate between that of MgO and that of bulk Ag. The presence of only one peak in the Ag scattering indicates that the Ag islands are coherent with the MgO.

1.2. Stage b: Dislocation formation

Around 4–6 ML, i.e., for an island width about 90 Å, an unusual change occurs: along both (H H 0.1) and (H 0 0.1) directions, the Ag peaks split into two components, one centered around the expected value ($H=2.06$) for fully relaxed Ag, and one centered around $H=2.03$. These two components grow with the deposited amount between 6 and 20 ML. We will show below that this phenomenon arises from the introduction of dislocations in the Ag islands. At this stage, the dislocations are not ordered.

The link between the introduction of misfit dislocations and the appearance of two peaks in the lattice parameter distribution of Ag can be understood intuitively. Indeed, in an island containing dislocations, Ag is under tensile strain parallel to the surface in regions located far from the dislocation cores, while it is under compressive strain in the dislocation core regions. In contrast, in an island without interfacial defects, Ag is under tensile strain everywhere.

1.3. Stage c: Ordering of dislocations.

Above 20 ML, the (2.03 2.03 0.1) peak continues to grow, while the (2.03 0.01) progressively disappears. This is typical of the formation of a network of misfit dislocations at the interface, as already reported in previous investigations.[13,18]

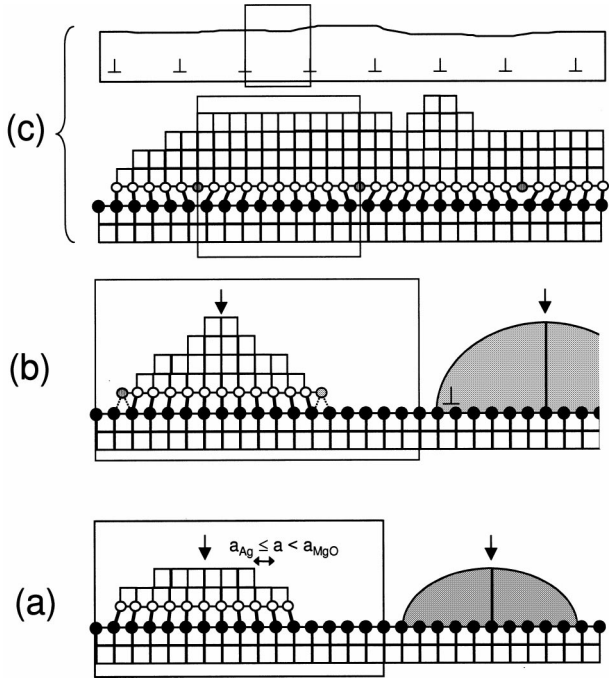

FIG. 5. Schematic representation of the morphology and structure during the first stages of growth of Ag on MgO(001) at room temperature, as a function of the amount of Ag deposited θ. A side view of the atomic positions within these islands is depicted. For all deposited amounts below 30 ML, the deposit consists in Ag islands with a height-over-width ratio of $\sim 0.37 \pm 0.05$. The growth is decomposed into three stages. (a) For $0 < \theta \leqslant 4-6$ ML, the Ag islands are coherent with the MgO. Their lateral size is smaller that 90 Å. Their in-plane lattice parameter is equal to that of bulk Ag at 0.5 ML, and then becomes intermediate between that of bulk Ag and that of MgO between 0.5 and 4–6 ML. (b) Around 4–6 ML, on the average, the islands reach a critical size ($\sim$90 Å) above which disordered misfit dislocations are introduced near their edges. (c) Above 30 ML, the film becomes continuous, and the dislocations reorder to form a square network. On all figures, the arrows locate the presence of a column in Ag that is exactly ''on site.'' The supercell used to calculate the crystal truncation rods is schematically shown.

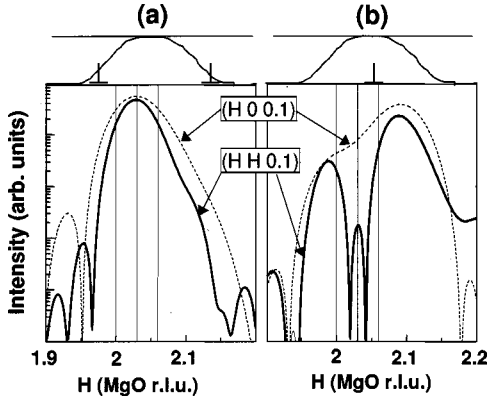

FIG. 6. Top: the different ways considered (side view) for positioning the Ag island, in the case of a semicoherent Ag/MgO interface. The misfit stresses at the interface between the Ag layer and the MgO substrate were supposed to be relaxed by the dislocation network described in [Refs. 37 and 38]. Two cases were considered: in case (a), the dislocation lines are located near the island edges, while in case (b), they are located at the center of the island. Bottom: corresponding radial scans along the (H H 0.1) (thick lines) and (H 0 0.1) (dashed lines) directions around $H=2$. An intermediate peak located around 2.03 along both directions is observed only in case (a) of dislocations near the edges.

We have recently shown[13] that these dislocations are oriented along $\langle 110 \rangle$ directions, with $\frac{1}{2}$ [110] Burger's vectors.

2. Simulation of the strain in Ag islands

This qualitative interpretation can be tested in a more quantitative way by calculating the atomic positions in a Ag island and deducing the corresponding radial scans. Numerical relaxation would be a method of choice, but, unfortunately, no simple form exists for the interatomic potentials in MgO and at the Ag-MgO interface. *Ab initio* methods cannot be used because the number of atoms to consider is too large. We thus resorted to simpler models.

The first stage of small islands coherent with the MgO can be simulated in a first approximation by using a linear elasticity calculation to determine the atomic positions in the coherent strained Ag island. This calculation was done using a finite-elements method,[36] assuming isotropic materials, a hemispherical Ag island (which is not too different from the actual average shape, and should thus be adequate for a first estimation) and a rigidity of the Ag-MgO bond equal to the rigidity of the Ag-Ag bond. Due to the symmetry, this calculation yields a central column of Ag atoms that is exactly ''on-site'' (i.e., registered) on the MgO substrate, the relaxation of Ag causing the atoms of the other columns to be displaced from the registered positions (see Fig. 5). These displacements increase with the radial distance from the center of the island. The intensity scattered by the island was then deduced by a Fourier transform. The calculated peak position ($H=2.047$) was found to be independent of the island size, provided the shape is kept constant. As for the experimental scans for $\theta < 4$ ML (Fig. 4), only one component is present in the calculated Ag peak.

Let us now explain the splitting of the Ag peaks during the second stage. By analogy with the satellite observed for very thick films,[13] it would be tempting to interpret the splitting of the Ag (220) peak as arising from the appearance of an interfacial dislocation network. However, the dislocation network does not yield any satellite at (2.03 0 0),[13] so this does not explain the splitting of the (200) Ag peak. We propose instead that the splitting of the Ag (220) and (200) peaks be indeed due to the introduction of misfit dislocations at the Ag/MgO interface, but that, at this stage, the dislocations are not ordered.

The introduction of discontinuities between the MgO and Ag lattices in the finite element calculation being quite difficult, a simpler approach was used. The incoherent Ag island was modeled (Fig. 6) by a Ag island cut in a bidimensional Ag layer presenting an ordered network of misfit dislocations at the Ag-MgO interface.[37] The atomic positions in the 2D layer were calculated using the linear-elasticity theory,[38] assuming a rigid substrate. A square lattice of edge dislocation lines, spaced by 97 Å and oriented along the $\langle 110 \rangle$ type directions, similar to that observed[13] for thick-Ag layers on MgO, was simulated. A Gaussian island shape was chosen, with a height given by the thickness of the layer

[$N=5$, 10 or 20 Ag (002) planes] and a FWHM fixed at 50 Å in order to avoid the effects due to the periodicity of the dislocations lattice. Whatever the location of the dislocation lines: near the edges [Fig. 6(a)] or centered [Fig. 6(b)], this model produces a component at $H=2.03$ along the (H H 0.1) direction. In order to also obtain a component at $H=2.03$ along the (H 0 0.1) direction, at least some of the Ag islands must have dislocation lines located near their edges [Fig. 6(a)]. This simulation therefore tends to confirm that the second component appearing around 4–6 ML in the Ag (220) and (200) Bragg peaks is due to the introduction of misfit dislocations that are not yet ordered. It also indicates that at least some of the dislocations are located at the edges of the islands.

C. Site and interfacial distance

1. Introduction

We have seen that, before dislocations are introduced, there are residual strains in the Ag islands. This implies that all interfacial Ag atoms are closer to a preferential substrate site, which we therefore call ''adsorption site.'' When atoms are displaced too much with respect to this site, interfacial dislocations are introduced, yielding ''good-match'' regions in which the adsorption site can still be defined, and ''bad-match'' regions in which the Ag atoms do not sit on top of any particular site. An important question is to determine the preferential adsorption site: is it above O ions of the substrate, above Mg ions or in between, above the octahedral site? Another important question is the average value of the interfacial distance, i.e., the distance between the last MgO plane and the first Ag plane.

Figure 7 shows the evolution with θ of the intensities along the (20L) and (11L) Mg OCTR's. A remarkable feature of the Ag/MgO growth is the drastic modification of the shape of the MgO CTR's induced by Ag deposition, even in very small amounts. It is shown below that this effect can be used to determine the adsorption site, the interfacial distance, and the morphology for very small deposited amounts, parameters that are impossible to deduce from measurements of the relaxed Ag Bragg peaks.

2. Origin of the interference

It is important to note that the MgO CTR's width in H and K is everywhere resolution limited, whatever the amount of Ag deposited.[39] This was deduced from radial and rocking scan measurements of the CTR's for the bare substrate, and for $\theta=2$ and 10 ML of Ag deposited. This observation allows to define in a general way what are the characteristics of the Ag causing the modifications of the MgO CTR's. The presence of interference along the MgO CTR's and the absence of evolution of their transverse width indicate that this phenomenon arises from Ag atoms that are correlated *via* the substrate over very long lateral distances, and have the substrate's correlation length (resolution limited). This corresponds to pairs of atoms whose in-plane separation is equal to exact multiples of the MgO lattice vectors, i.e., that have the same internal coordinate in the MgO unit cell (in prolongation of the MgO lattice inside the Ag). We call this fraction of the deposit ''substrate-correlated Ag fraction'' (SCF or SC Ag). Note that the Ag atoms of the SCF are not necessarily located above the MgO sites and do not necessarily form a continuous crystal.

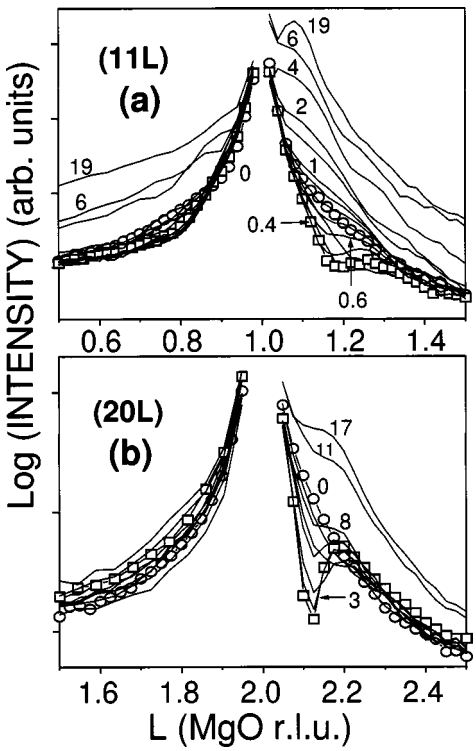

FIG. 7. Logarithm (Ref. 56) of the measured intensity along the (11L) (a) and (20L) (b) MgO CTR's, as a function of the out-of plane coordinate L, for different amounts of deposited Ag. Incident angle: 0.08° from 0 to 8 ML, 0.12° at 11 ML, 0.15° at 17 ML, and 0.22° at 19 ML. FIG. 6(a). (11L) CTR. Deposits: 0 ML (open circles), 0.2, 0.3, 0.4 ML (open squares), 0.5, 0.6, 0.7, 0.8, 0.9, 1, 1.5, 2, 4, 6, and 19 ML. FIG. 6(b). (20L) CTR. Deposits: 0 ML (open circles), 0.2, 0.5, 1, 2, and 3 ML (open squares) 4, 6, 8, 11, and 17 ML.

3. Simplified model

In a first crude approximation, we could consider that only the Ag atoms that are perfectly ''on-site'' contribute. The SCF would thus consist either in fully lattice-matched Ag, or in separated ''on-site'' columns that are located at the center of the islands during the first three stages of the growth, or exactly halfway between two dislocation lines when the film is continuous (see Fig. 5). In this last case, the SCF does not form a continuous crystal in the directions parallel to the surface, even on the scale of the interatomic spacing.

The MgO CTR's can be modeled by calculating the intensity scattered by the unit cell represented in Fig. 8. On the figure, Ag was supposed to sit on top of an oxygen site, but the site can of course be varied. The occupancy of the Ag plane located at a distance z from the last MgO plane is described by a complementary error function:

$$o(z)=o_{\mathrm{TOTAL}}\,\frac{1}{2N}\,\mathrm{erfc}\left(\frac{z-z_M}{\sqrt{2}.\sigma}\right),$$

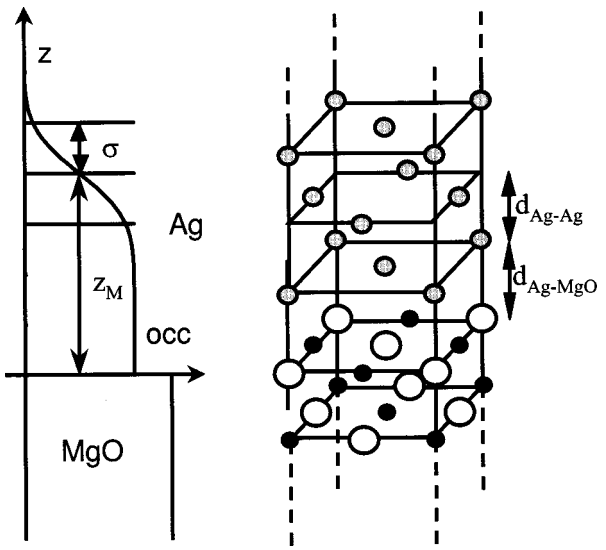

FIG. 8. Schematic drawing of the model used for fitting the CTR's. Right: atomic positions. Ag atoms are represented by gray circles, Mg ions by black disks, and oxygen ions by open circles. Left: shape of the profile describing the occupancy of the Ag planes as a function of the coordinate z perpendicular to the surface. In this figure, the substrate was supposed to be perfectly flat.

$$\text{where } N=\sum_{\substack{\text{Ag}\\ \text{plane}\\ \text{nbi}}} \frac{1}{2}\,\text{erfc}\left(\frac{z_i-z_M}{\sqrt{2}.\sigma}\right). \tag{1}$$

The parameters of this model (Fig. 8) are the ''total amount'' of SC Ag (o_{TOTAL}, in ML), the mean thickness of SC Ag domains, z_M, the additional roughness of the SC Ag with respect to the substrate, σ (which takes into account a possible dispersion in the height of the different domains of SC Ag), the interfacial distance $d_{\text{Ag-MgO}}$, and the average distance between two SC Ag planes, $d_{\text{Ag-Ag}}$, which is assumed here to be uniform. Such a model can easily be used for a quantitative analysis of the MgO CTR's, which is performed by refining the values of the parameters using a least-square fitting of the intensities.

4. Site, interfacial distance, and other structural parameters of the interface

Using this model, a qualitative analysis of the sign of the interference observed along the MgO CTR's shows that the Ag atoms of the first plane preferentially sit atop of the oxygen atoms of the last MgO plane.[10,11]

For a quantitative analysis of the CTR's, the experimental structure factors were deduced from the intensities measured either in L scans or by rocking scans, after normalization with respect to the incident flux, subtraction of the background measured on the clean MgO CTR's and application of the geometrical correction factors.[40] L-scans measurements can be used here because the resolution-limited width of the CTR's implies that the intensity at a given L position can be integrated without moving the sample.

The parameters of the model of Fig. 8 (o_{TOTAL}, z_M, σ, $d_{\text{Ag-MgO}}$, and $d_{\text{Ag-Ag}}$) and Eq. (1), represented in Fig. 9 as a function of θ, were determined by a simultaneous least-squares fit of the $(11L)$ and $(20L)$ CTR's. Figure 10 shows

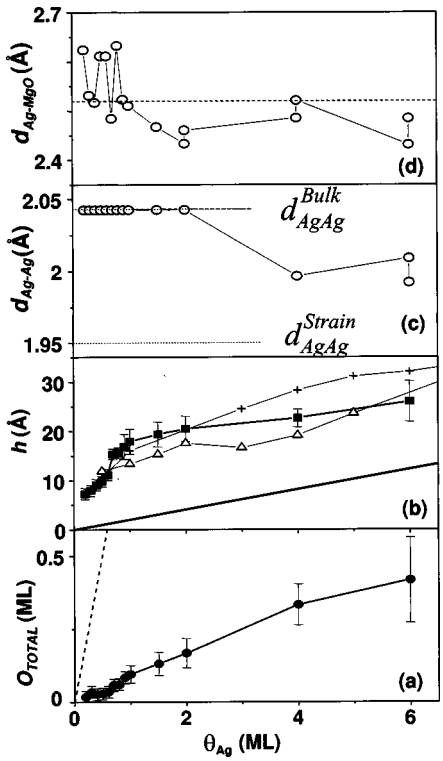

FIG. 9. Evolution with the amount θ of deposited Ag (in equivalent ML) of (a) the total amount of ''on-site'' Ag expressed in number of ML (solid circles with error bars), compared with the total amount deposited (dashed line), (b) the ''on-site'' Ag thickness (solid squares). It is compared with the average island height deduced from two independent GISAXS measurements with the 1D detector (crosses and open triangles). The total equivalent thickness of Ag deposited is also represented (solid line). (c): the interplane distance d_{AgAg} in Ag, perpendicular to the surface, compared with the distances $d^{\text{Bull}}_{\text{AgAg}}$ expected for bulk Ag, and $d^{\text{Strain}}_{\text{AgAg}}$ calculated according to isotropic elasticity for Ag strained in-plane to the MgO lattice parameter (dashed lines). (d) Interfacial distance $d_{\text{Ag-MgO}}$ deduced from the fits of the CTR's (open circles), and average interfacial distance (dashed line).

the comparison between the experimental CTR's and the best fits for selected deposited amounts θ. For the fits, the MgO(001) substrate was assumed to be unaffected by the Ag deposit. The scaling parameter and the substrate roughness were determined by a fit of the CTR's measured on the clean substrate, the substrate roughness (2.4 Å rms) being modeled by a Gaussian distribution of the terrace heights.[41] They were then fixed during the fits of the CTR's measured on the deposits of Ag on MgO.

The first striking feature is the very small amount of SC Ag [Fig. 9(a)]. It may be surprising that large effects are observed on the MgO(001) CTR's with such a small SCF amount. However, the MgO CTR's are extremely sensitive to the presence of Ag because its scattering power is 24 times that of MgO on the ''intense CTR's'' (H and K even, the MgO CTR intensity is proportional to the square of the sum of the atomic form factors of O and Mg), and 150 times that of MgO on the ''weak ones'' (H and K odd, intensity proportional to the square of the difference of the form factors of O and Mg).

The second important result is the large values of the height h of the SCF [Fig. 9(b)]. The very small amount of SC

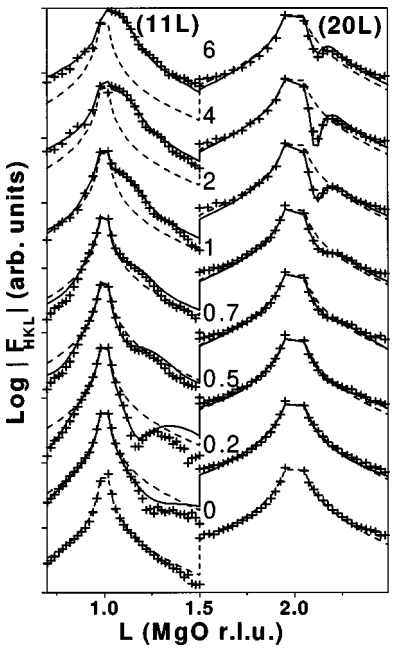

FIG. 10. Comparison between the measured (crosses) and calculated (solid lines) MgO CTR's during the room temperature growth of Ag on MgO(001). The logarithm (Ref. 56) of the modulus of the structure factor is plotted versus L. The dashed lines correspond to the clean MgO(001) substrate. The $(11L)$ and $(20L)$ CTR's have been represented on the same L scale although they are at different H, K values. The curves corresponding to the different amounts of deposited Ag are shifted vertically for clarity.

Ag (0.02 ML at $\theta = 0.2$ ML), and also the large values of h (about 3 planes at $\theta = 0.2$ ML) both confirm that the SCF does not consist in lattice-matched Ag. Indeed, if some lattice-matched Ag was present, it should be confined near the interface, so its thickness should not exceed one or two planes, and the major part of the first Ag plane would be lattice matched, which would yield an amount of ''on-site'' Ag close to the equivalent amount deposited θ, at least for small θ. The values found for h indicate that, already at 0.2 ML, Ag is in the form of islands with a height of several planes: there is no stage of two-dimensional growth. Additionally, from Fig. 9(b), for $\theta < 6$ ML, the thickness of the ''on-site'' Ag is practically equal to the average island height deduced from the GISAXS data. This agrees with the model of 3D growth proposed above, and confirms that the SCF extends from the interface to the surface of the islands, and that it is located near the center of the islands (i.e., near the point of maximal height).

However, although the SC Ag is not lattice matched, and extends over a significant height, it is not only composed of the central ''on-site'' columns either. Indeed, the amount of ''on-site'' Ag obtained with this simple model indicates that, whatever the island size, there is more than one ''on-site'' Ag column per island. At 6 ML, for instance, the occupancy of the first ''on-site'' plane is 0.05 ML, which, combined with an interisland distance of 150 Å and the hypothesis that there is one island every $(150\ \text{Å})^2$, leads to 125 ''on-site'' Ag columns per island.

5. General model

This observation led us to a more general model, in which, at least for $\theta < 4$ ML, we suppose that all the islands of Ag are *approximately* identical and ''pinned'' in the same way on the substrate (see Fig. 5 for a schematic picture), so that the whole Ag deposit contributes to the modifications of the MgO CTR's. In other words, we propose a model of partially relaxed islands correlated *via* the substrate. In such a model, where the SCF is the whole deposit, all the Ag atoms contribute to the MgO CTR's, but with a weight that decreases with increasing lateral separation from the central ''on-site'' column. In a small island of relaxed Ag, the central atomic column, which is perfectly ''on-site,'' fully contributes, because all the ''on-site'' columns are not only above MgO ones, but are in addition fully correlated via the substrate. As interfacial Ag atoms lie farther away from this central column, their contribution to the MgO CTR's decreases for two reasons. The first one is that they are more and more displaced from the ''on-site'' position. The second one is that pairs of atoms located in different islands far from the ''on-site'' column are less likely to be correlated by the substrate, because the exact atomic distribution presumably differs between different islands, especially if they are of different sizes.

Let us first illustrate this model by supposing that all the islands are *exactly* identical and ''pinned'' in the same way on the substrate. In this case, the MgO CTR's can be modeled by calculating the intensity scattered by a supercell that depends on the stage of the growth that is considered. For the stage (a) of the growth, the supercell (see Fig. 5) comprises a semi-infinite MgO column with a square basis (or hexagonal or circular, the exact shape is not very important) whose lateral size is equal to the interisland distance, and a Ag island that is either fully relaxed or slightly strained containing at its center a perfectly ''on-site'' column (Fig. 5). For stage (c) (continuous film with an ordered dislocation network), the unit cell is the supercell of the dislocation network. The case of stage (b) (islands containing dislocations) is intermediate.

A very simple estimation of the contribution of the Ag to the MgO truncation rods allows to predict the differences that will appear in the diffracted intensity between this new model and the first one. Let us assume for simplicity that all the Ag has its bulk lattice parameter, i.e., we model the $\theta = 0.5$ ML stage. The supercell comprises a semi-infinite column of MgO yielding a CTR centered on $\mathbf{Q}_{\parallel} = \mathbf{Q}_{\parallel \mathrm{MgO}}$, and a Ag island yielding a rod centered on $\mathbf{Q}_{\parallel} = \mathbf{Q}_{\parallel \mathrm{Ag}}$. The Ag rod, of width $2.\pi/d(\mathrm{FWHM})$, yields a contribution below the MgO CTR that decreases as the order of diffraction increases, since the spacing between the MgO and Ag rods increases with H and K while the width of the Ag peak remains constant. We experimentally observed this decrease of the Ag contribution along the CTR as a function of the rod order, which confirms the validity of this last model. By contrast, for lattice matched or ''on-site'' Ag, the respective weight of the Ag and MgO contributions to the MgO CTR would not vary with the order of the rod.

6. Validity of the interfacial parameters

One drawback of this general model is that it contains too many parameters for a quantitative analysis. Even if we were able to calculate the atomic positions in a Ag island given its size and shape, we would have to introduce as free parameters a mean island size, a mean shape, a mean interisland

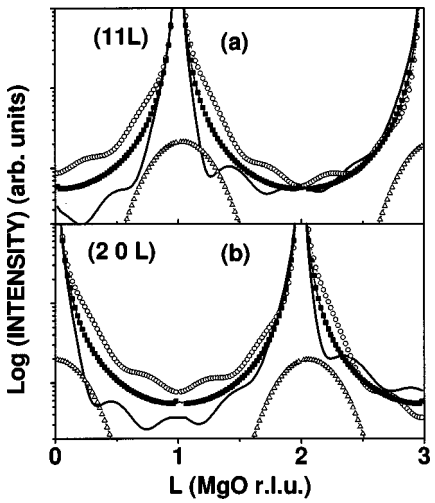

FIG. 11. Calculation of the intensity scattered along the $(11L)$ (a) and $(20L)$ (b) MgO CTR's, by a supercell composed of a semi-infinite MgO(001) substrate and a small hemispherical island of Ag at its bulk lattice parameter, with a 20-Å diameter. The logarithm (Ref. 56) of the intensity is plotted versus L. The interislands distance (i.e., the lateral size of the supercell) was fixed at 66 Å and the interfacial distance was fixed at the experimental steady-state value, 2.52 Å [Fig. 9(d)]. The MgO substrate contribution is shown as black squares and the Ag scattering as open triangles. For the $(11L)$ CTR (a), open circles show the CTR intensity for either a Mg or octahedral epitaxial site, and the thick line shows the intensity for an oxygen adsorption site. For the $(22L)$ CTR (b), the open circles correspond to the octahedral site, while the thick line shows the intensity for either an O or Mg site.

distance, and the dispersion over all these parameters, in order to estimate the Ag-Ag correlation function and derive the intensity. For the quantitative analysis of the MgO CTR's, the simpler model of ''on-site'' Ag was therefore used. Of course, this inadequately models the lateral position of the Ag atoms, but it allows to derive the interesting parameters: the height of the SCF, the adsorption site, the interplane distance in Ag, and the interfacial distance.

Let us first show that the adsorption site found with this simplified analysis corresponds to the real adsorption site. For this, we have calculated the intensity scattered by a supercell [MgO column+hemispherical Ag island, cf. Fig. 5(a)] for the extreme case where Ag has its bulk lattice parameter (stage $\theta=0.5$ ML). To make our simulation correspond approximately to the real situation at 0.5 ML, the lateral size of the island was taken equal to 20 Å, the interislands distance equal to 66 Å and the interfacial distance was fixed at the experimental steady state value, 2.52 Å [Fig. 9(d)]. Figure 11 shows the $(11L)$ and $(20L)$ CTR's calculated with the central atomic column of the symmetric island set either on top of O or Mg, or the octahedral site. The $(11L)$ CTR allows to distinguish between either the O site on the one hand, or the Mg or octahedral sites on the other hand, while the $(20L)$ CTR allows to distinguish between either the octahedral site on the one hand, or the O or Mg sites on the other hand. The clear destructive interference experimentally observed (Fig. 7) on both sides of the Bragg peaks along both CTR's is consistent only with the O site. The simulation with the O site (Fig. 11) qualitatively reproduces most of the observed interference at 0.5 ML. For the other sites, the simulated CTR's strongly differ from the experimental ones.

Hence, this very simple simulation shows that, in this system, a qualitative inspection of the sign of the interference along the CTR's using the ''on-site'' model allows to determine correctly the adsorption site.

Given this verification, we have to consider that the values deduced for $d_{\text{Ag-Ag}}$ [Fig. 9(c)] and $d_{\text{Ag-O}}$ [Fig. 9(d)] are average values over the SCF, because these distances are probably nonuniform within a given island, and may vary slightly between islands of different sizes and different strain states. The value of the average height [Fig. 9(b)] is probably representative of the average height of the islands, since it is the central portion of the islands that contribute the most. This is indeed verified by the good match with the thickness deduced from GISAXS [Fig. 9(b)].

Finally, we do not attach a particular meaning to the total amount of ''on-site'' Ag [Fig. 9(a)], because this parameter serves to ''hide'' everything that is not modeled properly, like the real lateral position of the atoms in the islands, and the dispersion on this parameter from one island to the other.

IV. DISCUSSION: INTERACTION BETWEEN Ag AND MgO

A. Site and interfacial distance

The adsorption site found here, above O ions of the substrate, is in agreement with the results of all the recent calculations[5,31,32,42–47] and of a recent surface x-ray absorption spectroscopy study.[48] This result contradicts those of an earlier high-resolution transmission electron microscopy (HRTEM) study,[12] which concluded to the existence of both Mg and O sites because of the imaging of $\langle 100\rangle$ misfit dislocations. However, we have shown[13] that the actual $\langle 110\rangle$ orientation of the dislocations is consistent with the presence of only one adsorption site. Note that the difference in energy between adsorption above Mg and adsorption above O is calculated to be small, and hence is the difference in energy for different orientations of the dislocation network. This could explain the different orientation observed on a very thin sample by HRTEM.

Let us examine now the values of $d_{\text{Ag-Ag}}$ and $d_{\text{Ag-O}}$ [Figs. 9(c) and 9(d)]. Below 2 ML, these two parameters were found to be strongly coupled in the fits. However, good fits were obtained by fixing $d_{\text{Ag-Ag}}$ to the value for bulk Ag for $\theta<2$ ML, which is consistent with the fact that Ag is close to its bulk parameter in stage (a). Above 2 ML, these two parameters are well decoupled. The average interplane distance $d_{\text{Ag-Ag}}=2.00\pm0.02$ Å is intermediate between the value for bulk Ag ($d_{\text{AgAg}}^{\text{Bulk}}=2.043$ Å) and the value of $d_{\text{AgAg}}^{\text{Strain}}=1.950$ Å calculated from the linear elasticity theory for Ag strained in plane to the MgO lattice parameter. This value is reasonably close to the average out-of-plane Ag distance of 2.025 Å deduced from our finite-element calculation of the strains in an island.

The interfacial distance is found nearly constant, with an average value of $d_{\text{Ag-MgO}}=2.52\pm0.1$ Å which is very close to the most recent theoretical values, of 2.34,[5,31] 2.38,[5,31] 2.47,[44] 2.49,[32,49] 2.50,[44] 2.45 to 2.64 Å,[43] depending on the Ag coverage, 2.64 Å,[45,43] and 2.69 [46] as well as to the ex-

perimental value of 2.53 Å found both by HRTEM (Ref. 12) and surface-extended x-ray-absorption fine structure.[48]

These results on the epitaxial site and interfacial distance show that the most recent *ab initio* calculations predict these parameters correctly. One important remark is that most published theoretical calculations neglect the lattice parameter mismatch between Ag and MgO and assume perfectly ''on-site'' Ag atoms. By contrast, in the real situation, Ag is never completely strained to the MgO in-plane lattice parameter. Therefore, even if most of the Ag atoms are close to a particular adsorption site (except those near the dislocation cores), there are only a few that are perfectly ''on site.'' This means that to be accurate, theoretical calculations of the interfacial parameters *should* take into account the lattice parameter mismatch and allow slightly ''off-site'' Ag atoms.

B. Evolution of the strain in Ag islands from the first stages of growth to the introduction of dislocations

The growth model in three stages reported above clearly shows that, at all stages, the strain and the morphology are strongly correlated. The observed strain evolution is very unusual: the islands are initially unstrained, but, as they grow beyond a critical size, they become progressively strained and introduce misfit dislocations. How can we explain that the small islands are initially unstrained? Why do they next become strained? Why are dislocations introduced in islands that are already partially relaxed? Finally, why do these dislocations reorder? The elasticity calculation using finite elements presented in Sec. III B 2 is clearly unable to provide an explanation for those facts.

The mechanism leading to the observed features can be qualitatively understood by using a simple two-dimensional model of Frenkel-Kontorova type[50,51] to describe the Ag-MgO interaction. In this model (Fig. 12), the vertical positions of the atoms are fixed. The force, which tends to bring back the adsorbate atoms of the first plane on top of the substrate sites (supposed to be fixed) is described by a periodic potential as a function of the lateral coordinate parallel to the interface, and the Ag atoms are harmonically bound together. The interatomic force between the Ag adatoms tends to bring back the interatomic Ag-Ag distance to its bulk value ($d_{\mathrm{Ag}}^{\mathrm{Bulk}}=a_{\mathrm{Ag}}/\sqrt{2}$), while the adsorbate-substrate interaction tends to bring it back to $d_{\mathrm{MgO}}^{\mathrm{Bulk}}=a_{\mathrm{MgO}}/\sqrt{2}$. The amplitude of the adsorbate-substrate potential is related to the difference of adsorption energy between the preferential site (i.e., on top of oxygen) and the unfavorable sites (i.e., the octahedral site, between two oxygen sites along the $\langle 110\rangle$ directions). The strain state in the adsorbate is thus determined by the respective weights of the Ag-Ag and Ag-MgO bonds, and by the value of the lattice parameter misfit.

Remark that the Ag surface stress should in principle be taken into account. It generally leads to a contraction of small nonsupported clusters[52–54] and can make the ''effective misfit'' [55] between Ag and MgO depend on the size of the Ag islands. However, the neglect of the surface stress will not change the present qualitative interpretation.

Let us examine the order of magnitude of the different parameters that intervene in this Frenkel-Kontorova model. The adhesion energy between Ag and MgO (0.23 to 0.64 J/m^2 [Refs. 1,5,31,32,42–47,49]) is very small, even for Ag adsorbed on the preferential site (oxygen). The adsorption of Ag on MgO is usually described as physisorption,[43] with a mostly electrostatic bonding, containing only a very weak metallic/covalent component.[5,31,47] By contrast, the interatomic ''springs'' between the Ag atoms are quite strong, since the Ag-Ag adhesion energy is 1.36 J/m^2. The Ag-O bond is thus much weaker than the Ag-Ag bond. Therefore, the major part of the strains is not in Ag but at the interface, in the form of lateral shifts between the adsorbate atoms of the first plane and their adsorption site. In addition, the amplitude of the corrugation of the substrate-adsorbate potential in the Frenkel-Kontorova model, is also very small. Indeed, this amplitude is the difference between the adhesion energy for Ag above the unfavorable Mg or octahedral sites and the adhesion energy above O ($\sim$0.3 and $\sim$0.2 J/m^2, respectively).

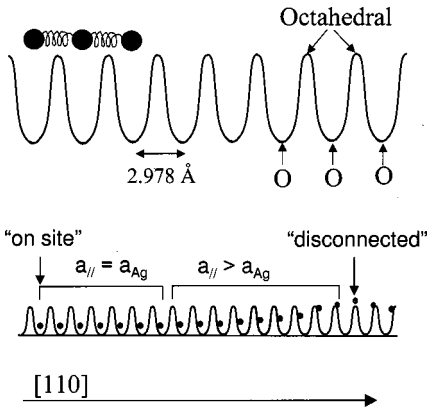

FIG. 12. Frenkel-Kontorova model of the Ag-MgO interface used to explain the evolution of strains in Ag during growth, i.e., as a function of increasing island size. The Ag-Ag bonds, which tend to bring back the Ag-Ag interatomic distance to its bulk value, are much stronger than the Ag-O bonds, which tend to bring back the Ag atoms on top of the oxygen sites. This, in addition with the very small amplitude of the interfacial potential corrugation, explains why very small islands remain unstrained, because the lateral displacements of interfacial atoms in the potential well result in a very small increase of interfacial energy. As the Ag islands get wider, their central atomic column stays in ''on-site'' position while the interfacial atoms at the edges get more and more displaced with respect to the bottom of the potential wells. The resulting increasing interfacial energy is released by a progressively increasing strain in the growing islands. The islands then reach a critical size at which the interfacial Ag atom at the edge is ''disconnected.'' This atom becomes the starting point of a misfit dislocation.

Figure 12 illustrates schematically the Frenkel-Kontorova model for the extreme case of a chain of Ag atoms with the interatomic spacing of bulk Ag. The farther the Ag atoms lie from the central ''on-site'' position, the more shifted they are with respect to the potential minimum, which causes an increase of the interfacial energy. The larger the islands, the larger the lateral shifts of the interfacial atoms located near the edge, and thus the larger the corresponding increase of interfacial energy. However, because the interaction of Ag and MgO is small and the amplitude of the interacting potential is small, even a large lateral displacement of the interfacial Ag atoms with respect to the potential minimum results only in a very small increase of the interfacial energy, compared to the Ag binding energy. In other words, the po-

tential well the Ag atom sits in on the MgO surface is flat enough in absolute value, compared to the Ag binding energy, to allow some latitude in the lateral position of the Ag atom relative to the O site on the MgO surface. As long as the islands are small enough, the total interfacial energy increase due to the cumulated lateral displacements of all interfacial atoms with respect to the potential minimum remains negligible with respect to the Ag binding energy. As a result, small Ag islands ''float'' on MgO with a weak attraction to sites above the O surface atoms and the Ag-Ag bonds in these islands are little affected by the substrate. This happens until the average island size reaches a critical value of $\sim$35 Å corresponding to $\theta = 1$ ML. When the island size increases above 35 Å, the ''line'' of interfacial Ag atoms becomes too long. If the Ag remained unstrained, the end Ag atoms would be located outside the potential well above the O atoms, and the increase of interfacial energy due to the cumulated lateral displacements of interfacial Ag would be too large. It becomes favorable to decrease the interfacial energy by pulling out the edge atoms into the potential well. These edges atoms are thus strained, which, in turn, tends to strain the whole island. The strained state in the Ag islands thus results from an equilibrium between the increase of Ag strain energy and the increase of interfacial energy due to the displacements of all interfacial Ag atoms with respect to the perfect ''on-site'' position. As the islands continue to grow, an intermediate state is found, with a small tensile strain in Ag and significant displacement of the edge atoms with respect to the potential well.

This naturally leads to the introduction of dislocations at the edges of the islands: an island will grow coherent with the substrate until it reaches a critical lateral size for which the atoms at the island edge (in a 2D model) sit halfway between two O sites, i.e., above the octahedral site along the $\langle 110 \rangle$ directions (see Fig. 12). As the island continues to grow, these atoms will stay ''disconnected'' from the substrate and the next atoms will be shifted by one site compared to the lattice-matched case (cf. Fig. 5). The ''disconnected'' atoms, on a barrier of the adsorbate-substrate potential, will tend to lie farther away from the MgO to minimize their energy. Each of these atoms will be the starting point of an interfacial misfit dislocation, which will build itself progressively as the island grows.

Hence, since the major part of the strains is not in Ag but at the interface, the appearance of dislocations does not correspond to a ''cracking'' of Ag islands accompanied with a reorganization (cutting and re-formation) of the adsorbate-substrate bonds as in the case of an initially lattice-matched deposit, but is rather a simple geometric effect.

For a Ag island with the lattice parameter of bulk Ag, the critical island size above which misfit dislocations are expected to appear is equal to the period of the coincidence site lattice between Ag and MgO, 97 Å. For an island that is partly strained, like at 3 ML, the critical size should be larger than 97 Å. Experimentally the average island size at which dislocations appear is about 90 Å, which is smaller than expected with this mechanism alone. This result is not completely understood.

In the above description of the way dislocations are introduced in an island, we have assumed for simplifying that the only process of island growth was the capture of individual Ag atoms. In fact, coalescence of neighboring islands is probably the main process of island growth, especially for strained islands, for which the capture of individual atoms at the island edges is energetically unfavorable. Let us consider what happens at the coalescence of two neighboring Ag islands that are coherent with the MgO and that have both an ''on-site'' column at their center. When these two islands coalesce, a defect appears at the region of contact since the centers of the two islands are not separated by exact multiples of Ag lattice vectors. The energy of this defect grows with the area of contact between the two islands, until it is large enough to make the resulting big island shift toward a configuration of smaller energy by a reorganization of the Ag-MgO bonds. One expects the energy to be lower if the defect migrates toward the edges of the resulting large island, where less atomic pairs will be affected by the strain field of the defect. If the resulting island is smaller than the period of the coincidence site lattice (CSL), the defect will simply disappear, and the island will become coherent with the MgO. If it is larger, it will end up as an incoherent island with dislocation lines near the edges. Therefore, the final state of the large island in this process (assuming that Ag has enough mobility) is the same as if the island had grown by capture of individual Ag atoms. To complete this description, in the case of coalescence of two islands already containing dislocations, one expects the reorganization of the Ag-MgO bonds to be mainly driven by the repulsion between the dislocations and the defect, combined with the repulsion between neighboring dislocations.

Finally, although complete *ab initio* calculations are not possible for large islands of Ag on MgO, our observation that there is no fully strained Ag is consistent with the only available *ab initio* calculation[44] that takes the misfit into account. Indeed, from this calculation, the energy per atom of a fully relaxed layer of five Ag atoms is 0.06 eV/atom lower than that of a fully strained film.

C. Ordering of interfacial dislocations

When the islands coalesce, the dislocations progressively reorganize into an ordered network because of the repulsive force between neighboring dislocations arising from the long-range strain field of the dislocations. The satellite peak around (2.03 0 0), which should vanish for a perfectly ordered network,[13] definitely disappears as the order builds in. At the same time, the satellite at (2.03 2.03 0) becomes progressively better defined.

V. CONCLUSIONS

In summary, for the growth of Ag on a clean and flat MgO (001) surface at room temperature with a deposition rate of 0.36 ML/min., we explain how the structure and morphology evolve as schematically shown in Fig. 5.

In agreement with the thermodynamic nonwetting character of the Ag/MgO interface, the growth proceeds by nucleation, growth, and coalescence of islands from the very beginning of the deposition (0.2 ML). The height-to-width ratio of the islands is nearly constant during growth, $\sim 0.37 \pm 0.05$. The film becomes practically continuous above 30 ML. Most of the Ag is in cube on cube epitaxy. A small

amount of twinned Ag also grows above 4 ML, as well as stacking faults above 10 ML.

A very unusual evolution of the strain state is observed with increasing amounts of Ag deposited. Below 1 ML, i.e., for an average in-plane island size smaller than 35 Å, the Ag islands are essentially unstrained. Between 1 and 4 ML, i.e., for island sizes between 35 and 90 Å, the Ag islands become more and more strained by the substrate, with a lattice parameter intermediate between those of bulk Ag and MgO. Around 4–6 ML, i.e., for an island size of the order of 90 Å, two peaks appear in the lattice parameter distribution of Ag, which arise from the formation of interfacial misfit dislocations at the Ag islands edges, driven by the fact that the islands reach a critical size of the order of the period of the coincidence site lattice. Above 30 ML, the interfacial dislocations reorganize into an ordered network, which has been evidenced elsewhere. [12,13]

This unusual evolution has been interpreted in terms of a very weak interaction between Ag and MgO, with rather flat potential wells: this makes very small islands ''float'' unstrained on the MgO surface, while wider islands get strained since the atoms at their edges sit on the steep portions of the interaction potential. The presence of relaxed Ag from the beginning of the deposition is consistent with the very small adhesion energy between Ag and MgO.

The epitaxial site is confirmed to be above O ions of the last MgO (001) plane, and the steady-state value of the interfacial distance for large deposited amounts is found to be $d_{\text{Ag-MgO}} = 2.52 \pm 0.1$ Å. These two results are consistent with all recent previous experimental determinations and theoretical predictions.

Concerning the technique of surface x-ray diffraction itself, this study shows that measurements of the substrate crystal truncation rods can be used to characterize the adsorbate even when the adsorbate does not contain a fully strained part.

ACKNOWLEDGMENTS

We would like to thank A. Bourret and I. K. Robinson for their critical reading of the manuscript, and J. Villain, C. Priester, C. Noguera, F. Lançon, and T. Deutsch for valuable discussions, and J. Jupille for his participation in one of the experiments.

*Author to whom correspondence should be addressed. FAX: 33 4 76 88 51 38. Present address: Materials Research Laboratory, University of Illinois at Urbana-Champaign, 104 South Goodwin Av., Urbana, IL 61801. Electronic address: grenaud@cea.fr

[1] M. W. Finnis, A. M. Stoneham, and P. W. Tasker, *Metal-Ceramic Interfaces*, Acta Scripta Metall. Proceedings Series Vol. 4 (Pergamon Press, New York, 1990).

[2] V. E. Henrich and P. A. Cox, *The Surface Science of Metal Oxides* (Cambridge University Press, Cambridge, 1994).

[3] *Proceedings of the International Symposium on Metal-Ceramic Interfaces* [Acta Metall. Mater. Suppl. 40 (1992)].

[4] C. Noguera, *Physics and Chemistry at Oxide Surfaces* (Cambridge University Press, Cambridge, 1996).

[5] J. R. Smith, T. Hong, and D. J. Slorovitz, Phys. Rev. Lett. **72**, 4021 (1994).

[6] P. Palmberg, T. Rhodin, and C. Todd, Appl. Phys. Lett. **11**, 33 (1967).

[7] A. K. Green, J. Dancy, and E. Bauer, J. Vac. Sci. Technol. **7**, 159 (1979).

[8] D. G. Lord and M. Prutton, Thin Solid Films **21**, 341 (1974).

[9] O. Robach, G. Renaud, and A. Barbier, Surf. Sci. **401**, 227 (1998).

[10] P. Guénard, Ph.D. thesis, Grenoble University, France, 1996.

[11] P. Guénard, G. Renaud, and B. Villette, Physica B **221**, 205 (1996).

[12] A. Trampert, E. Ernst, C. P. Flynn, H. E. Fischmeister, and M. Rühle, Acta Metall. Mater. **40**, S227 (1992).

[13] G. Renaud, P. Guénard, and A. Barbier, Phys. Rev. B **58**, 7310 (1998).

[14] F. H. Van der Merwe, Surf. Sci. **31**, 198 (1972).

[15] I. K. Robinson and D. J. Tweet, Rep. Prog. Phys. **55**, 599 (1992).

[16] J. R. Levine, J. B. Cohen, Y. W. Chung, and P. Georgopoulos, J. Appl. Crystallogr. **22**, 528 (1989).

[17] B. M. Lairson, A. P. Paine, S. Brennan, N. M. Rensing, and B. J. Daniels, J. Appl. Phys. **78**, 4449 (1995).

[18] O. Robach, G. Renaud, A. Barbier, and P. Guénard, Surf. Rev. Lett. **5**, 359 (1997).

[19] I. K. Robinson, Phys. Rev. B **33**, 3830 (1986).

[20] S. R. Andrews and R. A. Cowley, J. Phys. C **18**, 6247 (1985).

[21] http://www.esrf.fr

[22] A. K. Green, J. Dancy, and E. Bauer, J. Vac. Sci. Technol. **7**, 159 (1979).

[23] Y. Shigeta and K. Maki, Jpn. J. Appl. Phys. **16**, 845 (1977).

[24] F. Didier and J. Jupille, Surf. Sci. **307-309**, 587 (1994); F. Didier, Ph.D. thesis, University of Paris XI, 1994.

[25] K. Takayanagi, K. Yaki, and G. Honjo, Thin Solid Films **48**, 137 (1978).

[26] T. Harada, M. Asano, and Y. Mizutani, J. Cryst. Growth **116**, 243 (1992).

[27] D. Thiaudière, Ph.D. thesis, University of Poitiers, 1996.

[28] Although a priori valid only for a distribution of cylindrical clusters, this approximation was shown to yield a good estimation of the in-plane width for very different island shapes.

[29] H. Sato, S. Shinozaki, and L. S. Cicotte, J. Vac. Sci. Technol. **6**, 62 (1969).

[30] H. Sato and S. Shinozaki, Surf. Sci. **22**, 229 (1970).

[31] T. Hong, J. R. Smith, and D. J. Srolovitz, Acta Metall. Mater. **43**, 2721 (1995).

[32] J. Purton, S. C. Parker, and D. W. Bullet, J. Phys.: Condens. Matter **9**, 5709 (1997).

[33] A. Barbier, Surf. Sci. **406**, 69 (1998).

[34] B. E. Warren, Prog. Met. Phys. **8**, 146 (1959); M. S. Paterson, J. Appl. Phys. **23**, 805 (1952); A. J. C. Wilson, Proc. R. Soc. London, Ser. A **180**, 277 (1942).

[35] We have shown elsewhere (Ref. 13) that these rods cannot arise from facetted Ag and can only be attributed to stacking faults.

[36] D. Wong and M. D. Thoules, J. Mater. Sci. **32**, 1835 (1997).

[37] W. Bollmann, *Crystal Defects and Crystalline Interfaces* (Springer, Berlin, 1970).

[38] R. Bonnet, Philos. Mag. A **66**, 849 (1992).

[39] The clean MgO CTR's width was estimated at 0.01° from the width of a rocking scan around the (1 1 0.15) point. At this location, the width of the resolution function is negligible since

the Bragg angle is the same for the MgO and the monochromator.
[40] O. Robach, Ph.D. thesis, University of Grenoble, 1997.
[41] J. Harada, Acta Crystallogr., Sect. A: Found. Crystallogr. **48**, 764 (1992).
[42] P. Blöchl, G. P. Das, H. F. Fischmeister, and U. Schönberger, in *Metal-Ceramic Interfaces*, edited by M. Rühle, A. G. Evans, M. F. Ashby, and J. P. Hirth (Pergamon, Oxford, 1990), p. 9.
[43] E. Heifets, F. Y. Zhukovskii, E. A. Kotomin, and M. Causa, Chem. Phys. Lett. **283**, 395 (1998).
[44] L. Spiess, Surf. Rev. Lett. **3**, 1365 (1996).
[45] E. Heifets, E. A. Kotomin, and R. Orlando, J. Phys.: Condens. Matter **8**, 6577 (1996).
[46] C. Li, R. Wu, A. J. Freeman, and C. L. Fu, Phys. Rev. B **48**, 8317 (1993).
[47] H. X. Liu, H. L. Zhang, H. L. Ren, S. X. Ouyang, and R. Z. Yuan, Ceram. Int. **22**, 79 (1996).
[48] A. M. Flanck, R. Delaunay, P. Lagarde, M. Pompa, and J. Jupille, Phys. Rev. B **53**, R1737 (1996).
[49] U. Schönberger, O. K. Andersen, and M. Methfessel, Acta Metall. Mater. **40**, S1 (1992).
[50] J. Frenkel and T. Kontorova, Phys. Z. Sowjetunion **13**, 1 (1938).
[51] C. Ratsch and A. Zangwill, Surf. Sci. **293**, 123 (1993).
[52] G. Pacchioni and N. Rösch, J. Chem. Phys. **104**, 7329 (1996).
[53] V. Musolino, A. Selloni, and R. Carr, J. Chem. Phys. **108**, 5044 (1998).
[54] N. Rösch and G. Pacchioni, in *Chemisorption and Reactivity on Supported Clusters and Thin Films*, edited by R. M. Lambert and G. Pacchioni (Kluwer Academic, Dordrecht, 1997), p. 353.
[55] R. Kern and P. Muller, Surf. Sci. **392**, 103 (1997).
[56] Unless otherwise specified, the logarithm with base 10 is used in the figures.